MULTI-LAYER THIN-FILM MCM-D FOR THE REALIZATION OF Q- AND V-BAND FUNCTIONS

G. Carchon, S. Brebels, O. Vendier*, W. De Raedt

IMEC, div. MCP-MaRS, Kapeldreef 75, B-3001 Heverlee, Belgium
*Alcatel Space Industries, 26, Avenue J. F. Champollion, 31037 Toulouse, France
E-mail: geert.carchon@imec.be; Tel: ++32/(0)16/288191; Fax: ++32/(0)16/281501

Abstract — **We report on the mm-wave performance of a multi-layer thin-film MCM-D technology with integrated passive components. The standard 50 Ω CPW line exhibits a loss of -0.2 dB/mm at 60 GHz. A single CPW bridge (bend) has a return loss superior to -32 dB (-27 dB) up to 50 GHz with an insertion loss of -0.04 dB (-0.06 dB) at 50 GHz. A 30 GHz bandpass filter has achieved an insertion loss of -2.5dB over a 8% bandwidth with a return loss of -20 dB. A Q-band Wilkinson power divider has a return loss better than -15 dB from 31-48 GHz, isolation below -20 dB with an insertion loss of -3.5 dB. A quadrature coupler has a return loss better than -15 dB up to 60 GHz with an amplitude balance of 0.5 dB over the 38-60 GHz band, isolation of 20 dB, phase balance of (90+/-2)° and insertion loss of -4 dB.**

I. INTRODUCTION

The trend towards high-volume, low cost RF and microwave applications requires that suitable packaging techniques need to be developed. They should offer a high degree of integration to reduce size, weight, but also cost and power consumption. Multilayer thin-film multi-chip module technology (MCM-D) offers a very high reproducibility of small line dimensions (minimum feature sizes as small as 5 µm have been demonstrated [1]) and is therefore a promising technology for the low-cost integration of RF and microwave circuits.

Previously, a number of passive functions from RF to Ku band have been demonstrated [2-4]. Several circuits where the active components (e.g., a flip chipped bare-die component) and passive functions (using the MCM-D embedded passive components) are integrated on the same interconnect substrate, have been demonstrated in [5-7]. Here, we focus specifically on the mm-wave performance.

II. MCM-D TECHNOLOGY DESCRIPTION

IMEC's MCM-D layer built-up (Fig. 1) consists of alternating thin layers of BCB (benzo-cyclobutene, $\varepsilon_r = 2.65$) and Cu metallizations, deposited on a AF45 glass carrier substrate ($\varepsilon_r = 6.2$). The Cu layer (metal-2) is preferred for the realization of low loss CPW lines, however, the bottom (metal-1) and top (metal-3) layers can also be used. TaN-resistors with a typical value of 25 Ω/□ are integrated. For large capacitance values, anodized tantalum is used (720pF/mm^2), smaller capacitors (4.7 pF or 9.4pF/mm^2, depending on the type) are realized using BCB as insulating dielectric, or, below 100 fF, interdigital capacitors are used.

The quality factors of the inductors may go above 100 at 10 GHz (inductance < 1.7 nH). Naturally, for larger inductances a lower quality factor is obtained due to the increased losses and capacitive coupling between the turns, however, an 18 nH inductor still has a Q_{max} of 38 at 2 GHz while a 40 nH inductor Q_{max} of 29 at 1 GHz.

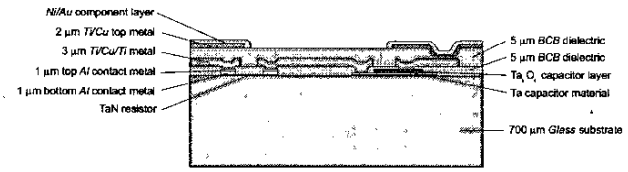

Fig. 1: Layer built-up of IMEC's MCM-D technology

As a planar technology is used, an MMIC type design methodology is used: all passive components and discontinuities have been modeled and integrated in a design library, hereby allowing to easily co-design several active and passive functions [8, 9].

III. TRANSMISSION LINE PERFORMANCE

As thin BCB layers are used, CPW transmission lines are preferred (as compared to thin-film microstrip lines) for the realization of low loss interconnects. The standard 50 Ω line is realized using a strip/slot of 77/20 µm and has a typical loss (Fig. 2) of -0.2 dB/mm @ 60 GHz. With 117µm as nominal ground-to-ground distance, CPW lines with characteristic impedances of 50-116Ω are feasible.

IV. DISCONTINUITIES

The optimization of discontinuities is especially important at mm-wave frequencies as the parasitic capacitances limit the high frequency performance of the technology.

A. Bridges

Grounding straps are required to suppress the excitation of the parasitic coupled slotline mode. Where airbridges are commonly used in CPW-based MMICs, bridges (on metal-3) or underpasses (on metal-1) can be used here.

The bridges used at RF-frequencies (Fig. 3 (a) and (b)), have a width of 40 µm, though, the associated parasitic

0-7803-7695-1/03/$17.00 © 2003 IEEE

capacitance to ground ($C_{g,par}$) is too high for mm-wave operation. $C_{g,par}$ may be reduced by reducing the width of the line, keeping the ground-to-ground spacing of the CPW line constant, however, the obtained capacitance reduction is limited due to BCB-planarization effects as shown in Fig. 4: as the strip width is reduced, the bridge comes closer to the signal, hereby increasing $C_{g,par}$.

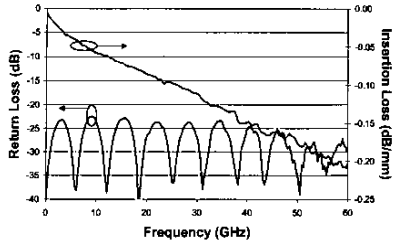

Fig. 2: Measured insertion loss and return loss for a 14 mm long 50 Ω line (width=77 μm, slot=20 μm).

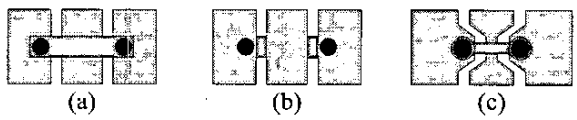

Fig. 3: Schematic layout of (a) the conventional bridge, (b) conventional tunnel and (c) optimized bridge structure.

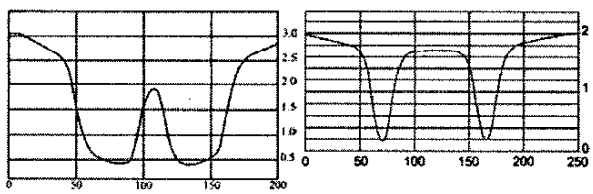

Fig. 4: Surface profile of a metal-2 CPW line with dimensions (a) slot/width=50.5/16 μm and (b) slot/width=77/20 μm.

The optimized bridge locally reduces the width, slot and bridge to 20 μm. The simulated performance (excluding planarization) of the different bridges is shown in Fig. 5: good performance of the optimized bridge may be observed.

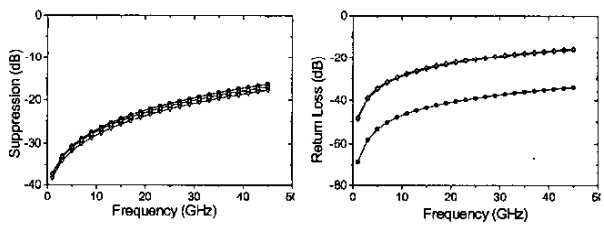

Fig. 5: Simulated performance (HFSS) of different bridge-types for a 50 Ω feeding line: (left) parasitic slotline mode suppression, (right) CPW mode return loss: (-Δ-) conventional tunnel, (-∇-) conventional bridge, (-•-) optimized bridge.

A transmission line is used to model the bridges. The parameters are determined by fitting the model to the measurements of a cascade of bridge-CPW sections (Fig. 6). The obtained result is shown in Fig. 7: the measured return loss of the cascaded structure is superior to -24 dB up to 50 GHz (return loss of a single bridge is superior to -32 dB up to 50 GHz). By comparing the measured loss of the cascaded structure with a CPW line, the insertion loss per bridge is in the order of -0.04 dB @ 50 GHz.

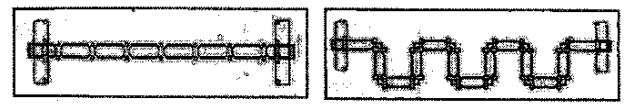

Fig. 6: Bridge and bend characterization test structures.

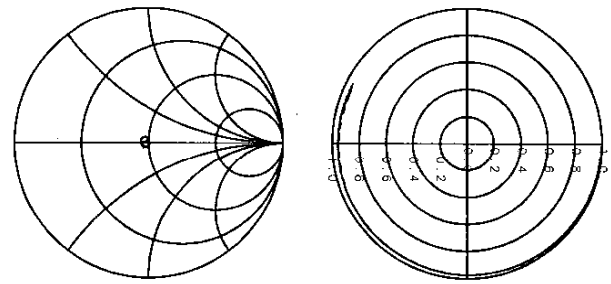

Fig. 7: Measured (black) versus modeled (grey) S_{11} (left) and S_{21} (right) of a cascade of seven optimized bridges and six 50 Ω CPW line sections (45 MHz - 50 GHz).

B. *Bends*

The layout is based on the above bridge layout and modeled as a short transmission line. The model parameters are determined by fitting the model to a cascade of bend-CPW sections as shown in Fig. 6, the obtained result is shown in Fig. 8: the return loss of the cascaded structure is superior to -22 dB up to 50 GHz. The insertion loss is in the order of -0.06dB/bend @ 50 GHz, whereas the return loss for a single bend is below -27 dB up to 50 GHz.

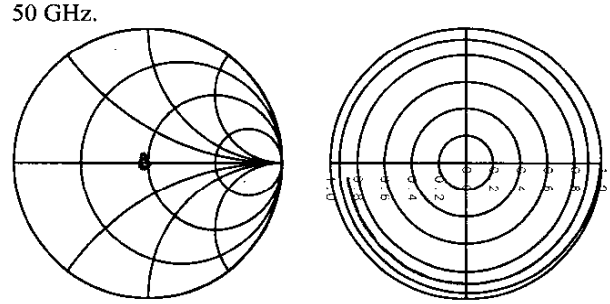

Fig. 8: Measured (black) versus modeled (grey) S_{11} (left) and S_{21} (right) of a cascade of 12 bends and 13 50 Ω CPW line sections.

C. *T-junction*

The layout of the T-junction is shown in Fig. 9. The characterization is based on [10]: the orthogonal port is terminated by 3 different "known" reflects: an open, a short and a 50 Ω load.

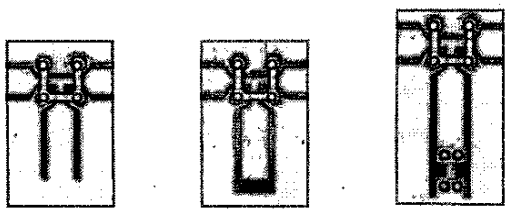

Fig. 9: Optimized T-junctions with 3rd port terminated in 3 different reflects: a short, an open and a 50 Ω load.

V. Q-BAND WILKINSON POWER DIVIDER

A Wilkinson power divider (Fig. 10) has been designed at 40 GHz: the measured return loss (Fig. 11) is better than -15 dB from 31-48 GHz, isolation (Fig. 12) better than -20 dB with an insertion loss of -3.5 dB.

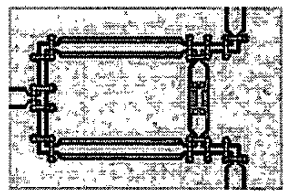

Fig. 10: 40 GHz Wilkinson power divider (0.6 x 1.2 mm^2).

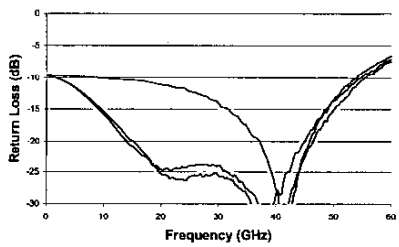

Fig. 11: Return loss of the 40 GHz Wilkinson power divider.

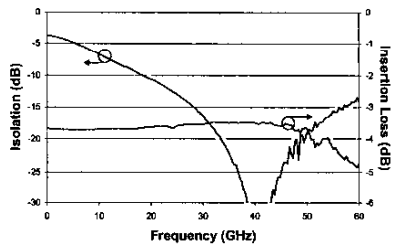

Fig. 12: Isolation and insertion loss of the 40 GHz Wilkinson power divider.

The measurements were obtained by repeating the structure 2 times on the wafer, terminating the orthogonal port in an on-wafer 50 Ω load. The effect of the non-ideal termination has been removed from the measurements using [11].

VI. Q-BAND QUADRATURE COUPLERS

As a 2-fingered 3-dB edge-coupled coupler matched to 50 Ω resulted in unfeasible dimensions, 70 Ω has been used as reference impedance in the following designs (the measurements have been renormalized accordingly). Version (a) in Fig. 13 uses two coupled lines (W=40μm, S=5 μm, S_{ground}=100 μm, coupling length 1mm), version (b) uses the same lateral dimensions, though the coupling is increased by two 75μm long floating patches on metal-3 at the edges of the coupler (overall coupling length of 875 μm). This method may further be used to increase the isolation at a specific frequency [4, 12].

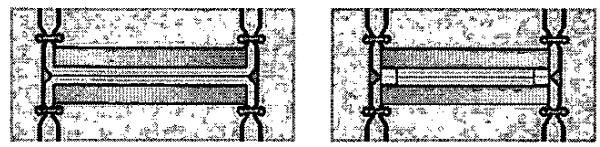

Fig. 13: Picture of (a) 2 finger quadrature coupler, (b) 2 finger quadrature coupler using additional capacitive coupling.

Version (a) achieves a return loss (Fig. 14) better than -15 dB up to 60 GHz with an amplitude balance of 0.5 dB over the 38-60 GHz band, isolation (Fig. 15) of 20 dB, phase balance of (90+/-2)° and insertion loss of -4 dB.

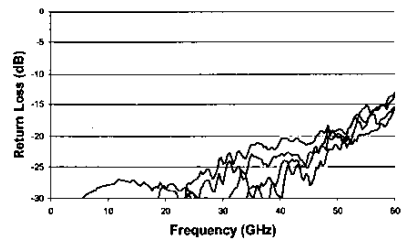

Fig. 14: Return loss of the 2-finger quadrature coupler.

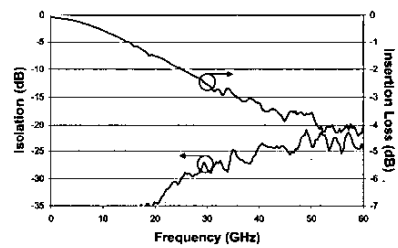

Fig. 15: Isolation and insertion loss of the 2-finger coupler.

Version (b) (Fig. 16, Fig. 17) has a return loss better than -15 dB up to 58 GHz, with an amplitude balance of 1 dB over the 31 to +60 GHz band, phase balance of (90+/-2)°, worst case isolation and insertion loss of 17 dB and -4.4 dB, respectively.

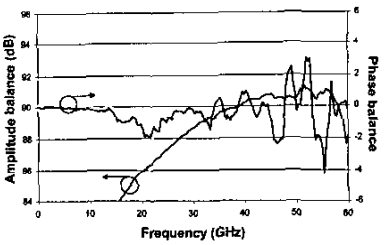

Fig. 16: Amplitude and phase balance of the 2-finger quadrature coupler using additional broadside coupling.

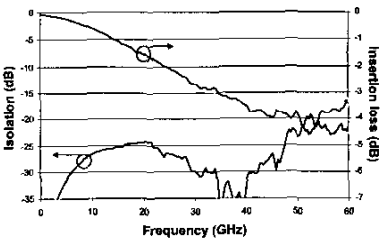

Fig. 17: Isolation and insertion loss of the 2-finger quadrature coupler using additional broadside coupling.

VII. Integrated Attenuators

Attenuators can be integrated in the MCM-D technology. The measured performance of a 3dB, 6dB and 9 dB attenuator is given in Fig. 18.

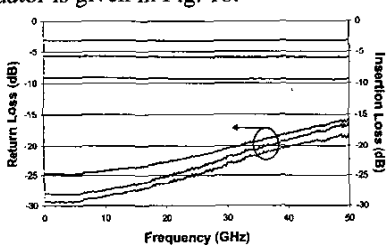

Fig. 18: Measured return loss and insertion loss for a 3 dB, 6dB and 9 dB attenuator.

VIII. Ka-band Bandpass Filter

A Ka-band band-pass filter is shown in Fig. 19: an insertion loss of -2.5 dB over a 8 % bandwidth has been obtained at 30 GHz. The measured return loss is -20 dB.

IX. Conclusions

We have reported on the mm-wave performance of a multi-layer thin-film MCM-D technology with integrated passives. The standard 50 Ω CPW line exhibits a loss of -0.2 dB/mm at 60 GHz. Several circuits have been realized: a 30 GHz bandpass filter achieved an insertion loss of -2.5 dB over a 8% BW with a return loss of -20 dB. A Q-band Wilkinson power divider has a return loss better than -15 dB from 31-48 GHz, isolation below -20 dB with an insertion loss of -3.5 dB. A quadrature coupler has a return loss better than -15 dB up to 60 GHz with an amplitude balance of 0.5 dB over the 38-60 GHz band, isolation of 20 dB, phase balance of (90+/-2)° and insertion loss of -4 dB.

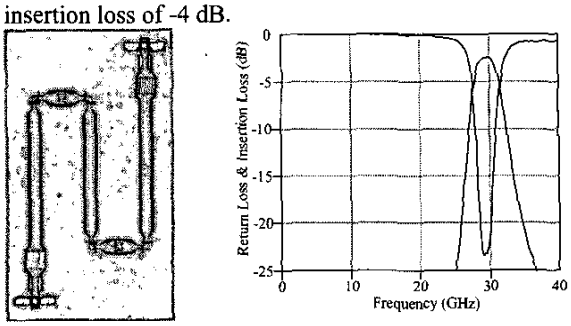

Fig. 19: Ka band bandpass filter using 3 coupled CPW line sections, and 4 interdigital capacitors.

Acknowledgements

The authors acknowledge the support from the European Commission under the MIPA project (IST-2000-28276). The authors also thank the ACOSTE processing team for the realization of the thin-film technology.

References

[1] G. Carchon, et al., "Spiral inductors in multi-layer thin-film MCM-D," *IMAPS Europe*, Poland, pp. 255-260, 2002.

[2] G. Carchon, et al., "Integrated Wilkinson Power Dividers in C-, Ku- and Ka-band in Multi-Layer Thin-Film MCM-D," *European Microw. Conf.*, France, pp. 171-174, 2000.

[3] G. Carchon, et al., "Multi-layer thin film MCM-D for the integration of high-performance wireless front-end systems," *Microwave Journal, vol. 44, pp. 96-110, 2001.*

[4] G. Carchon, et al., "Integration of CPW Quadrature Couplers in Multi-Layer Thin-Film MCM-D," *IEEE Trans. on MTT*, vol. 49, pp. 1770-1776, 2001.

[5] G. Carchon, et al., "Chip-MCM co-design of a 14 GHz LNA," *Int. Conf. on HDIP*, pp. 64-69, April 17-20, 2001.

[6] G. Carchon, et al., "A Direct Ku-band Linear Subharmonically Pumped BPSK and I/Q Vector Modulator in Multi-Layer Thin-Film MCM-D," *IEEE Trans. MTT*, vol. 49, pp. 1374-1382, 2001.

[7] K. Vaesen, et al., "Chip-Package Co-Design of a 4.7 GHz VCO," *Int. Jour. Microc. and Elec. Pack.*, vol. 23, pp. 272-279, 2000.

[8] G. Carchon, et al., "Novel approach for a design-oriented measurement-based fully scalable coplanar waveguide transmission line model," *IEE Proc. Microw. Antennas Propagation*, vol. 148, pp. 227-232, 2001.

[9] G. Carchon, et al., "Multilayer Thin-Film MCM-D for the Integration of High-Performance RF and Microwave Circuits," *IEEE Trans. on CPaT*, vol. 24, pp. 510-519, 2001.

[10] G. Carchon, et al., "Accurate measurement and characterization of reciprocal 3-ports, application to CPW T-junctions in thin-film multi-layer MCM-D," *Asia Pacific Microw. Conf.*, pp. 453-456, December 3-6, 2000.

[11] J. C. Rautio, "Techniques for correcting scattering parameter data of an imperfectly terminated multiport when measured with a two-port network analyzer," *IEEE Trans. on MTT*, vol. 31, pp. 407-412, 1983.

[12] M. Dydyk, "Microstrip directional couplers with ideal performance via single-element compensation," *IEEE Trans. on MTT*, vol. 47, pp. 956-964, 1999.